Int. J. Electrochem. Sci., 12 **(2017)** 5000 – 5011, doi: 10.20964/2017.06.29

International Journal of ELECTROCHEMICAL SCIENCE
www.electrochemsci.org

Synthesis and Electropolymerization of Furan End−capped Dibenzothiophene/Dibenzofuran and Electrochromic Properties of Their Polymers

Hua Gu[1,‡], *Kaiwen Lin*[2,‡], *Hongtao Liu*[3], *Nannan Jian*[3], *Kai Qu*[3], *Huimin Yu*[3], *Jun Wei*[3], *Shuai Chen*[1,4,*] *and Jingkun Xu*[1,4,*]

[1]School of Pharmacy, Jiangxi Science & Technology Normal University, Nanchang 330013, PR China
[2]School of Materials Science and Engineering, South China University of Technology, Guangzhou 510641, PR China
[3]School of Chemistry & Chemical Engineering, Jiangxi Science & Technology Normal University, Nanchang 330013, PR China;
[4]Jiangxi Engineering Laboratory of Waterborne Coatings, Nanchang 330013, PR China
[*]E−mail: chenshuai@ms.xjb.ac.cn, xujingkun@jxstnu.edu.cn
‡ These authors contributed equally to this work.

Received: 20 January 2017 / *Accepted:* 18 April 2017 / *Published:* 12 May 2017

Two furan end−capped dibenzo five−membered ring monomers, 2,8−bis−(furan−2−yl)−dibenzothiophene (DBT−Fu) and 2,8−bis−(furan−2−yl)−dibenzofuran (DBF−Fu) were successfully synthesized via Stille couple reaction. Corresponding polymers, P(DBT−Fu) and P(DBF−Fu), were obtained by employed the electropolymerization. The surface morphology, electrochemical and optical properties of monomers and polymers were researched by cyclic voltammetry (CV), scanning electron microscopy (SEM), and UV−via spectra method. Both polymers exhibited obvious color changes from neutral state to oxidation state (from green−yellow to dark grey for P(DBT−Fu) and from beige to celadon for P(DBF−Fu)).

Keywords: conducting polymers, furan, dibenzothiophene/furan, electropolymerization, electrochromism

1. INTRODUCTION

Conducting polymers have drawn great attention in electrochromic filed because of the dual advantages of traditional polymer materials and new semiconductor materials.[1−2] Among them, dibenzo five−membered ring−heterocycle hybrid polymers exhibited good processibility, tunable electronic and optical properties *via* feasible functionation.[3−8] In the past decades, most attention has

been concentrated on polyfluorenes, polycarbazole and their derivatives because of easy functionalization at the 9 positions, fine solution−processability, high stability, multi–color, and perfect redox activity.[9−11] However, the close analogs of fluorene–carbazole, dibenzothiophene (DBT) and dibenzofuran (DBF) were with limited attention and less reported in electrochromic filed. In contrast, due to their rigid planarity and excellent fluorescence properties, DBT and DBF have been significantly investigated in solar cells and sensors.[3,12] From 2014, our group subsequently studied the electrochromic properties of thienyl and its homologues end−capped dibenzothiophene and dibenzofuran.[13,14] Among them, DBT−3HexTh exhibited a better performance (69 % of optical contrast and 330 cm^2 C^{-1} of coloration efficiency in UV field). Experiments indicated that DBT and DBF were good electrochromic candidate. Polyfuran was more environmentally friendly hybrid compound than polythiophene.[15−16] Due to the poor stability in reaction or environment, a very limited number of studies were taken out to furan.[17,18] In 2006 Tovar and coworkers[19] synthesized a novel D–A–D skeleton utilized furan as donor unit for the first time and studied their electrochemical properties in detail. Subsequently, Woo et al.[20] found that furan−based hybrid polymers exhibited similar electrical and optical properties compared to their thiophene counterparts. Recently, Önal et al. synthesized three conjugated hybrid polymers based on furan and fluorene units with quasi−reversible redox behavior and satisfied electrochromic behaviors.[22] These reported polymers (as shown in **Scheme 1**) illustrated if polyfuran being inserted into building block of hybrid polymers, its shortcome can be overcome to obtain satisfied electronic and optical performance.

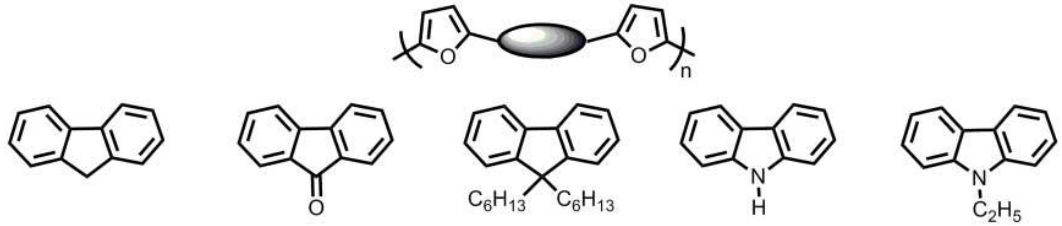

Scheme 1. The representative structures of furan end−capped dibenzo five−membered ring−heterocycle hybrid polymers

Herein, we designed and synthesized two novel conjugated hybrid monomers (as shown in Scheme 2) 2,8−bis−(furan−2−yl)−dibenzothiophene (DBT−Fu) and 2,8−bis−(furan−2−yl)−dibenzofuran (DBF−Fu) employing furan as end−capping unit and dibenzothiophene and dibenzofuran as dibenzo pentacyclic centers *via* Stille coupling reaction. We investigated the electropolymerization of monomers and their electrochemical, optical, and electrochromic properties of corresponding polymers.

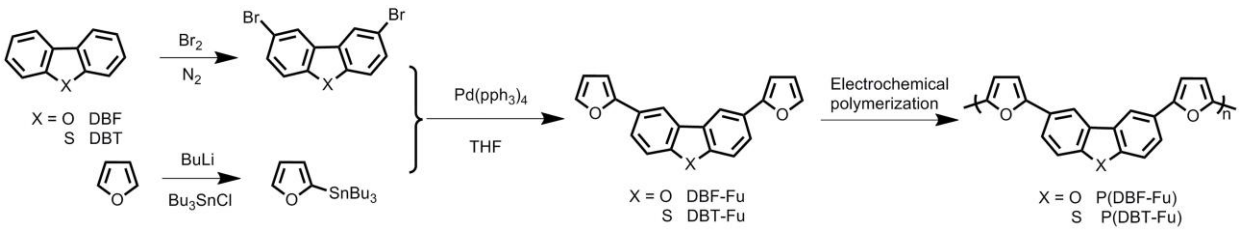

Scheme 2. Synthetic routes of DBT−Fu, DBF−Fu and corresponding polymers.

2. EXPERIMENTAL SECTION

2.1 Chemicals

DBT (99%; Energy Chemical), DBF (99%; Energy Chemical), furan (99%; TCI) was stored at 0 °C before use. Tetrabutylammonium hexafluorophosphate (Bu_4NPF_6, 98%; Energy Chemical) and 1−butyl−3−methylimidazolium hexafluorophosphate ($BmimPF_6$, 98%; Energy Chemical) were used directly. Dichloromethane (CH_2Cl_2, analytical grade), acetonitrile (ACN, analytical grade), and tetrahydrofuran (THF, analytical grade) were purchased from Shanghai Vita Chemical Ltd and used after reflux distillation. Unless there was a special note, other chemicals and reagents were all analytical grade and used directly.

2.2 Monomer synthesis

2.2.1 Synthesis of 2,8−dibromodibenzothiophene and 2,8−dibromodibenzofuran.

The synthesis of 2,8−dibromodibenzothiophene and 2,8−dibromodibenzofuran were following previously reported literature.[13−14]

2,8−dibromodibenzothiophene: a white powder with 85% yield. ^{1}H NMR (400 MHz, $CDCl_3$, ppm): δ 7.38 (d, J = 12.2 Hz, 2H), 7.52 (d, J = 7.8 Hz, 2H), 8.05 (d, J = 4.4 Hz, 2H).

2,8−dibromodibenzofuran: a white solid with yielded 75%. ^{1}H NMR (400 MHz, $CDCl_3$, ppm): δ 7.44 (d, J = 8.0 Hz, 2H), 7.57 (d, J = 8.6 Hz, 2H), 8.03 (d, J = 3.8 Hz, 2H).

2.2.2 Synthesis of tributyl(furan−2−yl)stannane

Under nitrogen atmosphere, *n*−BuLi (9.0 mL, 1.6 mol L^{-1} in hexane) was added dropwise to flask containing furan (1.02 g, 0.015 mol) and refined THF (15.0 mL) through an addition funnel. The reaction mixture was stirred for 1~2 h at −78 °C, and then chlorotributyltin was added dropwise by the same method at −40 °C for another 4 h. After that, the reaction mixture was stirred at room temperature overnight. Then the solvent was removed by rotary evaporation and used for the following steps without other farther purification.[23,24]

2.2.3 Synthesis of 2,8−bis(furan−2−yl)−dibenzothiophene (DBT−Th)

15 mL refined THF, 2,8−dibromodibenzothiophene (1.00 g, 2.9 mmol), and tributyl(furan−2−yl)stannane (5.20 g, 14.5 mmol) were added to a two necked flask. And then $Pd(PPh_3)_4$ dissolved in THF was injected though partition as the catalyst. The mixture maintained reflux status under constant stirring and nitrogen atmosphere for 24 h. After that, the reaction mixture was cooled down to room temperature and extracted by CH_2Cl_2 to collect organic layer. And then the solvent was removed by rotary evaporation. Finally, the purified pale yellow powder with 73% yield was obtained by used column chromatography. ^{1}H NMR (400 MHz, $CDCl_3$, ppm): δ 8.54 (s, 2H), 7.85

(d, *J* = 8.4 Hz, 2H), 7.80 (dd, *J* = 12.8 Hz, 2H), 7.57 (s, 2H), 6.81 (d, *J* = 4.0 Hz, 2H), 6.57 (m, *J* = 8.3 Hz, 2H).

2.2.4 Synthesis of 2,8−bis(furan−2−yl)−dibenzofuran (DBF−Fu)

The synthetic method of DBF−Fu was similar to that of DBT−Fu. The final product was yellow powder with 65% yield. ^{1}H NMR (400 MHz, $CDCl_3$, ppm): δ 8.30 (d, *J* = 4.6 Hz, 2H), 7.80 (d, *J* = 4.8 Hz, 2H), 7.56 (d, *J* = 24.6 Hz, 2H), 7.52 (s, 2H), 6.70 (d, *J* = 4.0 Hz, 2H), 6.53 (m, *J* = 4.0 Hz, 2H).

2.3 Electrochemistry and Characterization

Electrochemical behaviors of monomers and polymers were studied by employing Model 263A potentiostat–galvanostat (EG&G Princeton Applied Research) under computer control. Two polished Pt wires were used as working electrode and counter electrode, respectively. An homemade Ag/AgCl electrode prepared in 6 M HCl solution was used as reference electrode. The electrodes were placed away from each other during the experiments. All of experiments were performed at room temperature under oxygen free environment. In order to get adequate amount of the polymer film, ITO−coated glass was utilized as the working electrode with a surface area of 5 cm × 0.8 cm. Before used, the ITO glass was immersed in ethanol, cleaned by ultrasonically wave and then dried in air.

NMR spectra were recorded *via* Bruker AV 400 NMR spectrometer with $CDCl_3$ as the solvent and tetramethylsilane as an internal standard. Scanning electron microscopy (SEM) measurements were obtained using JSM 6701F scanning electron microscope. UV−vis spectra were recorded through Perkin−Elmer Lambda 900 Ultraviolet−Visible Near−Infrared spectrophotometer.

3. RESULTS AND DISCUSSION

3.1 Synthesis of DBT−Fu and DBF−Fu

As shown in **Scheme 2**, dibenzothiophene/ dibenzofuran were brominated with Br_2 in chloroform/glacial acetic acid to obtain 2,8−dibromodibenzothiophene/2,8−dibromodibenzofuran, respectively.[13,14] And then, DBT−Fu and DBF−Fu were successfully obtained by employing Stille coupling reaction with tributyl(furan−2−yl)stannane and 2,8−dibromodibenzothiophene or 2,8−dibromodibenzofuran using $Pd(PPh_3)_4$ as catalyst. Considering the unstability of terminal furan, both monomers were stored in a refrigerator (4 °C).

3.2 Electrochemical behavior of DBT−Fu and DBF−Fu

As shown in **Figure 1** and **Table 1**, the onset oxidation potential (E_{onset}) of DBT−Fu (0.98 V) was a bit lower than that of DBF−Fu (0.99 V), which may arise from the lower polarisability of an

oxygen atom (O) in the structure of DBF in contrast to DBT monomer with sulfur atom (S) in structure.[25] Also, those values were lower than that of DBT−Th and DBF−Th.[13] Due to the electronegativity of O atoms from end−copped Fu unit leads to larger electron cloud density and lower oxidation potential of DBT−Fu and DBF−Fu. The existence of FOF with 9−fluorenone as core also proved this theory.[26] Such lower oxidation potential of monomer benefits to yield higher quality polymers and relatively narrow band gap.

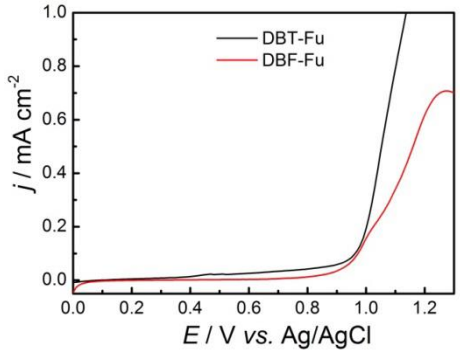

Figure 1. Anodic polarization curves of 0.1 M DBT−Fu and DBF−Fu in CH_2Cl_2−Bu_4NPF_6 (0.10 M). Potential scan rates: 50 mV s^{-1}.

3.3 Electrochemical polymerization of DBT−Fu and DBF−Fu

Cyclic voltammetry (CV) in three−electrode system is good strategy to expose the process of electrochemical polymerization and electrochemical activity. In view of the solubility of polymer films, THF−Bu_4NPF_6 (0.10 M) was used as electrolyte solution to perform the electrochemical study.

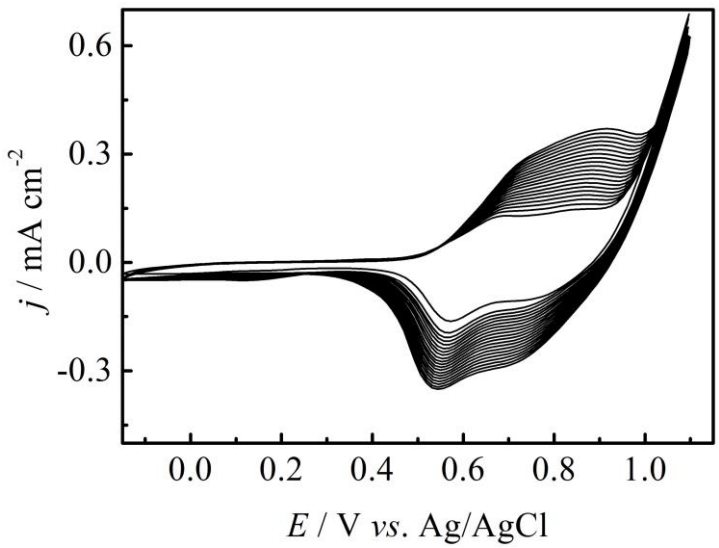

Figure 2. Electropolymerization of 0.1 MDBT−Fu in THF−Bu_4NPF_6 (0.10 M). Potential scan rates: 50 mV s^{-1}.

Figure 2 showed the CV curves of DBT−Fu with potential range from –0.15 V to 1.10 V. A pair of reversible redox peaks occurred between 0.50 V and 0.70 V, which account for the reverse scanning of the current density is higher than the positive scanning in the first circle because of nucleation.[27] With increasing of current density, P(DBT−Fu) films were progressively deposited on the surface of the electrode with dark−grey color. Moreover, the redox peak potential was shift to higher, which was due to the increasing of resistance. Because of the rigid structure and instability of furan and harsh electropolymerization conditions of BDF−Fu, we were not able to get the CV curve.

Table 1. Electrochemical and optical properties for DBT−Fu, DBF−Fu, P(DBT−Fu), and P(DBF−Fu).

Sample	$\lambda_{max,1}$ (nm)	$\lambda_{max,2}$ (nm)	HOMO (eV)	LUMO (eV)	$E_{ox,onset}$ (V)	$E_{g,opt}$ (eV)	Ref
DBT−Th	271	307	−5.92	−2.37	1.12	3.55	[4,13]
P(DBT−Th)	410	540	–	–	–	2.53	
DBF−Th	263	301	−6.01	−2.74	1.21	3.27	
P(DBF−Th)	392	588	–	–	–	2.41	
FOF	–	–	–	–	1.36		[26]
PFOF	–	350	−5.20	−2.88	–	2.32	
DBT−Fu	270	305	−5.77	−2.04	0.98	3.73	This work
P(DBT−Fu)	–	330	−5.00	−2.47	–	2.53	
DBF−Fu	262	288	−5.72	−2.21	0.99	3.51	
P(DBF−Fu)	–	320	−5.10	−2.48	–	2.62	

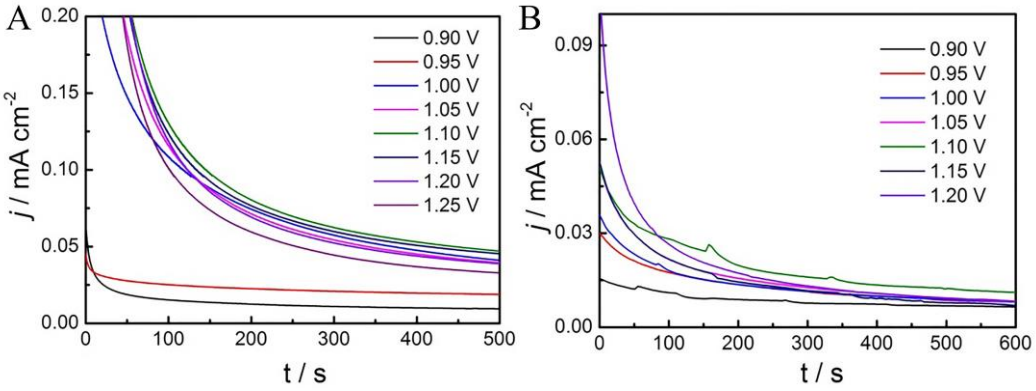

Figure 3. Chronoamperometric curves of the monomers DBT−Fu and DBF−Fu in CH_2Cl_2−Bu_4NPF_6 (0.10 M) on Pt electrodes at different applied potentials.

Deposition potential has great effect on the quality and performance of the conjugated polymer film.[28] Therefore, a set of applied potentials in CH_2Cl_2–Bu_4NPF_6 (0.1 M) as shown in Figure 3 were studied to optimize the electropolymerization potential. When the applied potentials do not reach the E_{onset}, the surface of the electrode has no polymer formation. Which was mainly contributed the low current densities. With the applied potential increasing, the current density and the mass of the polymer films increase correspondingly. However, the current density decreased rapidly and crossed in the other current density curves at applied potentials. This phenomenon can be seen as over−oxidation.

Considering the moderate polymerization rate, quality of polymers, regular morphology, and good adherence, the optimized applied potential of 1.10 V vs. Ag/AgCl was chosen for both monomers.

3.4 Electrochemical behavior of polymers

In order to explore the electroactivity of polymers deposited on Pt electrodes, the CVs were studied from 0.2 to 1.2 V for P(DBT−Fu) and from 0.3 to 1.1 V for P(DBF−Fu) in monomer−free electrolytes, respectively. As shown in Figure 4, a couple of redox peaks seated at 1.75 ~ 1.07 V and 0.54 ~ 0.96 V were observed for P(DBT−Fu). Whereas the redox peaks located between 0.90 V and 0.45 V could be seen for the P(DBF−Fu). The difference between P(DBT−Fu) and P(DBF−Fu) revealed the influence of the structural changes of central atom (from S to O). In addition, the broad redox peaks of P(DBT−Fu) indicated it has more charge trapping and electron withdrawing ability than P(DBF−Fu).[19,20] The linear relationships between the scan rate and the peak current density (Figure 4C and 4D) illustrated that the polymer films were well adhered on the electrode and the redox processes were non−diffusion controlled.[29,30]

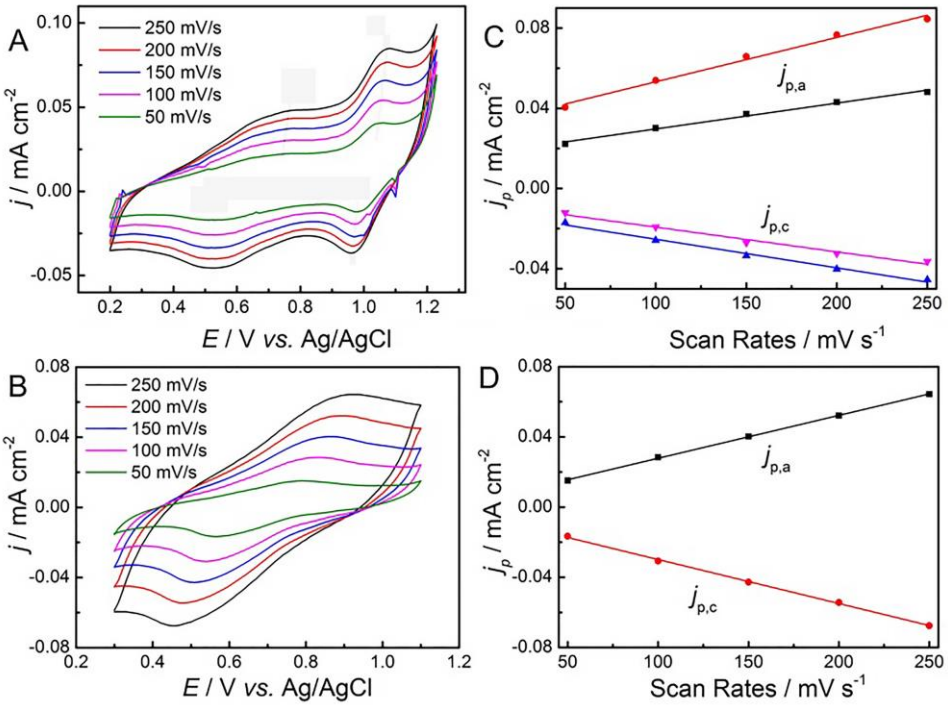

Figure 4. CVs of P(DBT−Fu) films (A) and P(DBF−Fu) films (B) at different scan rates between 50 and 300 mV s^{-1} in the monomer−free 0.1 M ACN–Bu_4NPF_6 solution. The scan rate dependence of the anodic and cathodic peak current densities graph of P(DBT−Fu) (C) and P(DBF−Fu) (D).

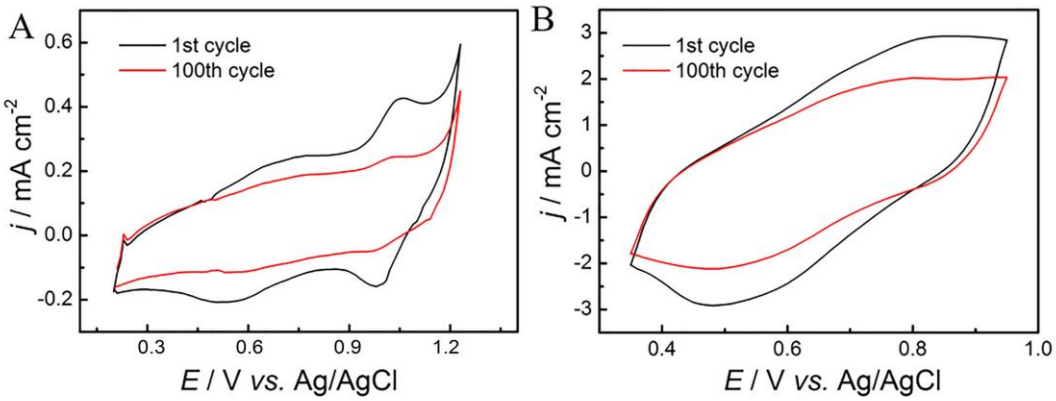

Figure 5. Redox stability of P(DBT−Fu) films (A) and P(DBF−Fu) films (B), cycled 100 times with a scan rate of 150 mV s^{-1} in the monomer−free 0.1 M ACN−Bu_4NPF_6 solutions.

Redox stability is a crucial factor for electrochromic polymers. The electrochemical stability were studied by CVs with potential from 0.2 V to 1.2 V for P(DBT−Fu) and from 0.35 V to 0.95 V for P(DBF−Fu). As shown in Figure 5, P(DBF−Fu) exhibited better stability with 22% loss of its electroactivity after sweeping 100 cycles. While P(DBT−Fu) was remained 75 % of the exchange charge after sweeping 100 cycles. The reasons for the fast decrease of electrochemical activity were as follow: (1) strong polarity of organic solvents (ACN); (2) instability of furan in conducting structure.[31,32]

3.5 Optical and morphology of polymers

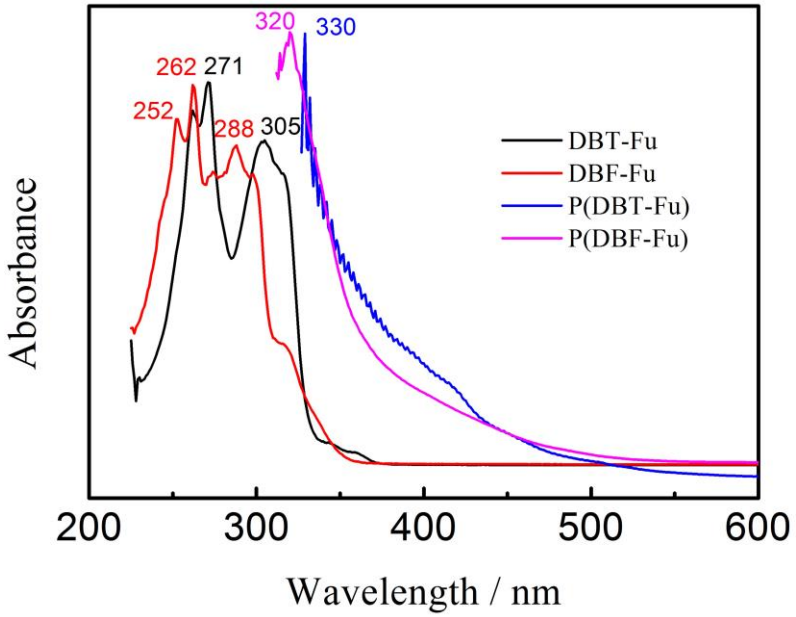

Figure 6. UV−vis absorbtion spectra of monomers in CH_2Cl_2−Bu_4NPF_6 solution and corresponding polymers in $BminPF_6$.

UV–visible spectrum is usually utilized to interpret the electronic properties of electrosynthesized polymers. As seen in Figure 6, when comparison each other, DBT−Fu exhibited two characteristic absorbance peaks at 271 nm and 305 nm respectively and DBF−Fu revealed two blue−shifted absorption peaks at 262 nm and 288 nm respectively. What is more, two monomers revealed different on LUMO, which was due to the core of dibenzo five−membered ring monomer with different hibrid atom in building block. [4,22] The same situation applies to the monomers with same end−capped units.[4,13−22] In comparison with corresponding polymers, P(DBT−Fu) have a absorbance peaks at 330 nm and P(DBF−Fu) was at 320 nm, which was mainly assigned to long conjugation length of polymers. Otherwise, P(DBF−Fu) was blue−shifted about 10 nm than that of P(DBT−Fu) and 30 nm than that of P(FOF)[26] because of the influence of different hibrid atom. According to the onset of the π−π* transition, the $E_{g,opt}$ values of polymers (as shown in Table 1) were 2.53 eV for P(DBT−Fu) and 2.62 eV for P(DBF−Fu). The $E_{g,opt}$ value of P(DBT−Fu) was higher than that P(DBT−EDOT) (2.46 eV),[14] but lower than that P(DBT−Th) (2.53 eV) [13], which were due to the different ability of rich electronic capacity.

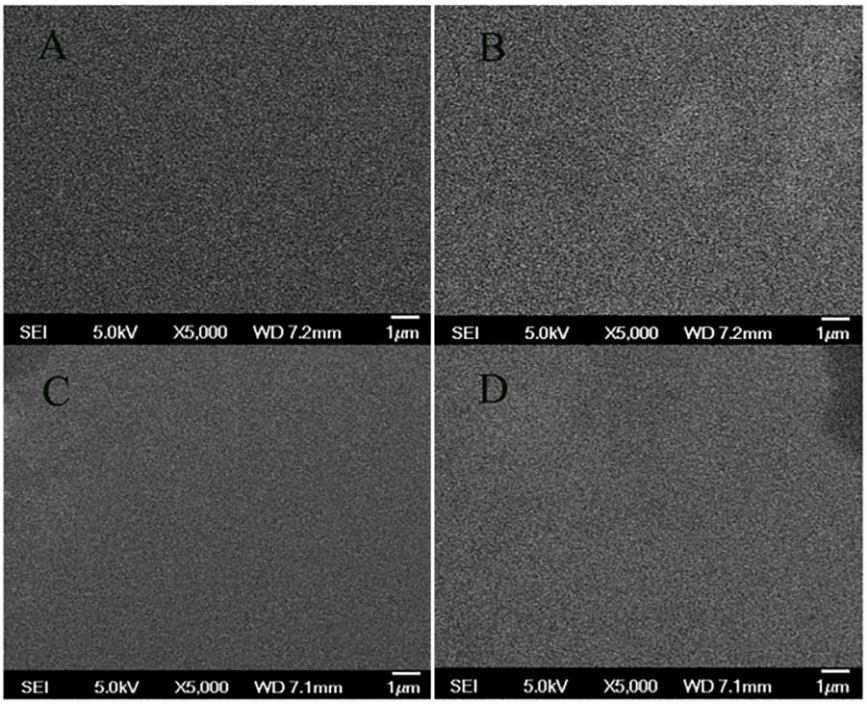

Figure 7. SEM of (A) dedoped and (B) doped P(DBT−Fu) films, (C) dedoped and (D) doped P(DBF−Fu) films deposited potentiostatically onto ITO glass at 5000 times.

Figure 7 showed that P(DBT−Fu) and P(DBF−Fu) had smooth surface morphology both in doped and dedoped states at 5000 times. The doped P(DBT−Fu) films dissolved into electrolyte and P(DBF−Fu) film became rough at doped state. These phenomena were mainly due to the immigrations/emigrations of counterions, which destroyed the polymer morphology in the doped/dedoped processes.[33] The same situation occured in many SEM of polymer structures. But, compared with P(DBT/F−EDOT) and P(DBT/F−Th), the stability and performance of P(DBT−Fu) and

P(DBF−Fu) film were bad, which ascribe to 1) rigid structure of polymers; 2) instability of furan structure.

3.6 Electrochromic performance of polymers

The spectroelectrochemical properties of P(DBT−Fu) and P(DBF−Fu) were measured under different potentials with $BminPF_6$ as electrolyte solvent due to the good solubility of both polymers. Considering the π–π* transition, the absorption peak occurred at 320 nm for P(DBT−Fu) and 330 nm for P(DBF−Fu) at reduced state, respectively. Stronger rigid structure and richer electronic properties render the UV−vis spectra of P(DBF−Fu) red−shifted. With the potential increasing, new and broad absorption peaks between 500 ~ 800 nm were appeared for both polymers. The above mentioned phenomenon was due to the presence of polaron.[34]

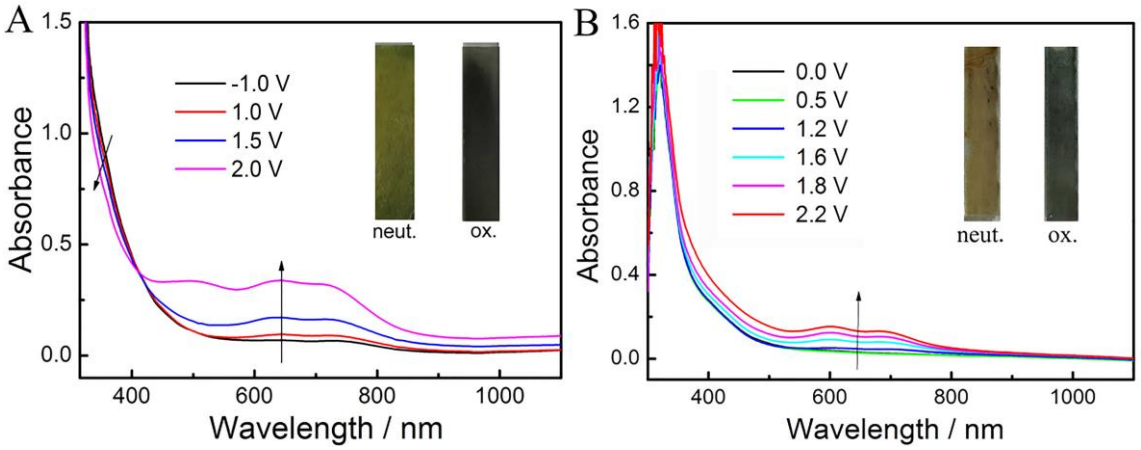

Figure 8. Spectroelectrochemical spectra of (A) P(DBT−Fu) film and (B) P(DBF−Fu) film on ITO electrode under applied potentials between –1.0 V and 2.0 V for (A), 0.0 V and 2.2 V for (B) in monomer−free BminPF6 solutions.

Table 2. Electrochromic parameters of P(DBT−Fu) and P(DBF−Fu).

Polymers		CIE color coordinates		Colors of polymers	
		Neutral	Oxidized	Neutral	Oxidized
P(DBT−Fu)	L*	97.63	89.97		
	a*	–1.23	–0.56		
	b*	6.45	1.31		
P(DBF−Fu)	L*	95.01	88.37		
	a*	–3.85	–4.78		
	b*	6.70	0.63		

Color changes of polymer films between redox states were recorded by camera. At the same time, the *CIE* 1976 (L^*, a^*, b^*) shown in Table 2 was employed to accurately detect the change of color at the micro level. The polymers of P(DBT−Fu) were changed from green–yellow (L^*: 97.63, a^*: –1.23, b^*: 6.45) to dark grey (L^*: 89.97, a^*: –0.56, b^*: 1.31), while the color changed from beige (L^*: 95.01, a^*: –3.85, b^*: 6.70) to celadon (L^*: 88.37, a^*: –4.78, b^*: 0.63) for P(DBF−Fu) films between neutral and oxidized state. Through the color changing of polymer films, we believe that P(DBT−Fu) and P(DBF−Fu) are good candidates of electrochromic materials, but also provides a valuable basis for the study of dibenzo five−membered ring electrochromic materials

4. CONCLUSION

In summary, two novel dibenzo five−membered hybrid monomers, DBT−Fu and DBF−Fu have been successfully synthesized and their polymers were obtained by electropolymerization. Due to the different structures, the electrochemical and electrochromic performances were obviously different for P(DBT−Fu) and P(DBF−Fu). DBT−Fu had lower onset oxidation potential and easier electropolymerization than DBF−Fu. In addition, P(DBT−Fu) film not only had better adhesion, stability, and lower optical band gap than P(DBF−Fu), but also possessed much gorgeous color changes from green−yellow to dark grey between neutral state and oxidation state. The black and green electrochromic materials are the pursuit of electrochromic field. Through development of DBT and DBF, it was expected to achieve high quality and black electrochromic materials which is quite useful for the field of display.

ACKNOWLEDGEMENTS
We are grateful to the National Natural Science Foundation of China (No. 51463008 and 51603095), Science Foundation for Excellent Youth Talents in Jiangxi Province (No. 20162BCB23053), Key Project of Jiangxi Educational Committee (No. GJJ150795), Jiangxi Educational Committee for a Postgraduate Innovation Program (No. YC2016−S410), Scientific Fund of Jiangxi Science & Technology Normal University (No. 2014QNBJRC003 and 2016QNBJRC003), Jiangxi Science & Technology Normal University Program for Scientific Research Innovation Team (No. 2015CXTD001), Scientific Research Foundation for Doctors in Jiangxi Science & Technology Normal University (2015), and Undergraduate Entrepreneurship Research Fund (2016) for their financial support of this work.

References

1. H. Shirakawa, E.J. Louis, A.G. Macdiarmid, C.K. Chiang, A.J. Heeger, *Chem. Commun.* 16 (1977) 578.
2. Y.P. Zou, A. Najari, P. Berrouard, S. Beaupre, R.B. Aich, Y. Tao, M. Leclerc, *J Am Chem Soc* 132 (2010) 5330.
3. U. Posset, M. Harsch, A. Rougier, B. Herbig, G. Schottner, G. Sextl. *RSC Adv* 2 (2012) 5990.
4. K.W. Lin, S. Chen, B.Y. Lu, J.K. Xu, *Sci. China Chem.* Doi: 10.1007/s11426−016−0298−2 (2016)
5. S. Koyuncu, O. Usluer, M. Can, S. Demic, S. Icli, N.S. Sariciftci, *J. Mater. Chem.* 21 (2011) 2684.

6. F.B. Koyuncu, S. Koyuncu, E. Ozdemir, *Org. Electron.* 12 (2011) 1701.
7. F. B. Koyuncu, S. Koyuncu, E. Ozdemir, *Electrochim. Acta* 55 (2010) 4935.
8. B. Liu, W. L. Yu, Y. H. Lai, W. Huang, *Chem. Mater.* 13 *(*2001) 1984.
9. P.M. Beaujuge, J.R. Reynolds, *Chem. Rev.* 110 (2010) 268.
10. B.Y. Lu, Y.Z. Li and J.K. Xu, J. *Electroanal. Chem.* 643 (2010) 67.
11. W.Q. Zhou, J.K. Xu, Z.H. Wei, S.Z. Pu, *Chin. J. Polym. Sci.* 26 (2008) 81.
12. O. Usluer, S. Koyuncu, S. Demic, R.A.J. Janssen, *J. Polym. Sci., Part A: Polym. Chem.* 49 (2011) 333.
13. K.W. Lin, S.L. Ming, S.J. Zhen, Y. Zhao, B.Y. Lu, J.K. Xu. *Polym. Chem.* 6 (2015) 4575.
14. K.W. Lin, S.J. Zhen, S.L. Ming, J.K. Xu, B.Y. Lu. *New J. Chem.* 39 (2015) 2096.
15. S.J. Zhen, J.K. Xu, B.Y. Lu, S.M. Zhang, L. Zhao, J. Li, *Electrochim. Acta* 146 (2014) 666–678.
16. S.J. Zhen, B.Y. Lu, J.K. Xu, S.M. Zhang, Y.Z. Li, *RSC Adv.* 4 (2014) 14001.
17. A.T. Yiu, P.M. Beaujuge, O.P. Lee, C.H. Woo, M.F. Toney, J.M.J. Fréchet, *J. Am. Chem. Soc.* 134 (2012) 2180.
18. M. içli−özkut, H. ipek, B. Karabay, A. Cihaner, A.M. önal, *Polym. Chem.* 4 (2013) 2457.
19. K. Loganathan, P.G. Pickup, *Electrochim. Acta* 52 (2006) 15.
20. C.H. Woo, P.M. Beaujuge, T.W. Holcombe, O.P. Lee, J.M.J. Frechet, *J. Am. Chem. Soc.* 132 (2010) 15547.
21. X. Wang, S. Chen, Y. Sun, M. Zhang, Y. Li, H. Wang, *Polym. Chem.* 2 (2011) 2872.
22. A. Günes, A. Cihaner, A.M. Önal, *Electrochim. Acta* 89 (2013) 339.
23. G.E. Gunbas, A. Durmus, L. Toppare, *Adv. Mater*. 20 (2008) 691.
24. S.S. Zhu, T.M. Swager, *J. Am. Chem. Soc.* 119 (1997) 12568.
25. P. Camurlu, T. Duraka, A. Balan, L. Toppare, *Synth. Met.* 161 (2011) 1898.
26. A. Günes, A. Cihaner, A.M. Önal, *Electrochim. Acta* 89 (2013) 339.
27. G.M. Nie, H.J. Yang, S. Wang, X.M. Li, *Crit. Rev. Solid. State.* 4 (2011) 209.
28. B.Y. Lu, S.J. Zhen, S.M. Zhang, J.K. Xu, G.Q. Zhao, *Polym. Chem.* 5 (2014) 4896.
29. Z.P. Wang, J.K. Xu, B.Y. Lu, S.M. Zhang, L.Q. Qin, D.Z. Mo, S.J. Zhen, *Langmuir* 30 (2014) 15581.
30. B. Bezgin, A.M. Önal, *Electrochim. Acta* 55 (2010) 779.
31. W. Lu, A. G. Fadeev, B. Qi, E. Smela, B.R. Mattes, J. Ding, G.M. Spinks, J. Mazurkiewicz, D.Z. Zhou, G.G. Wallace, D.R. MacFarlane, S.A. Forsyth, M. Forsyth, *Science* 5583 (2002) 983.
32. W. Lu, A.G. Fadeev, B. Qi, E. Smela, B.R. Mattes, J. Ding, G.M. Spinks, Jakub. Mazurkiewicz, D.Z. Zhou, G.G. Wallace, D.R. MacFarlane, S.A. Forsyth, M. Forsyth, *J. Phys. Chem. B.* 1 (2002) 70.
33. S. Beyazyildirim, P. Camurlu, D. Yilmaz, M. Gullu, L, *J. Electroanal. Chem.* 587 (2006) 235.
34. J. Hwang, J.I. Son, Y.B. Shim, *Sol. Energy. Mater. Sol. Cells.* 94 (2010) 1286.